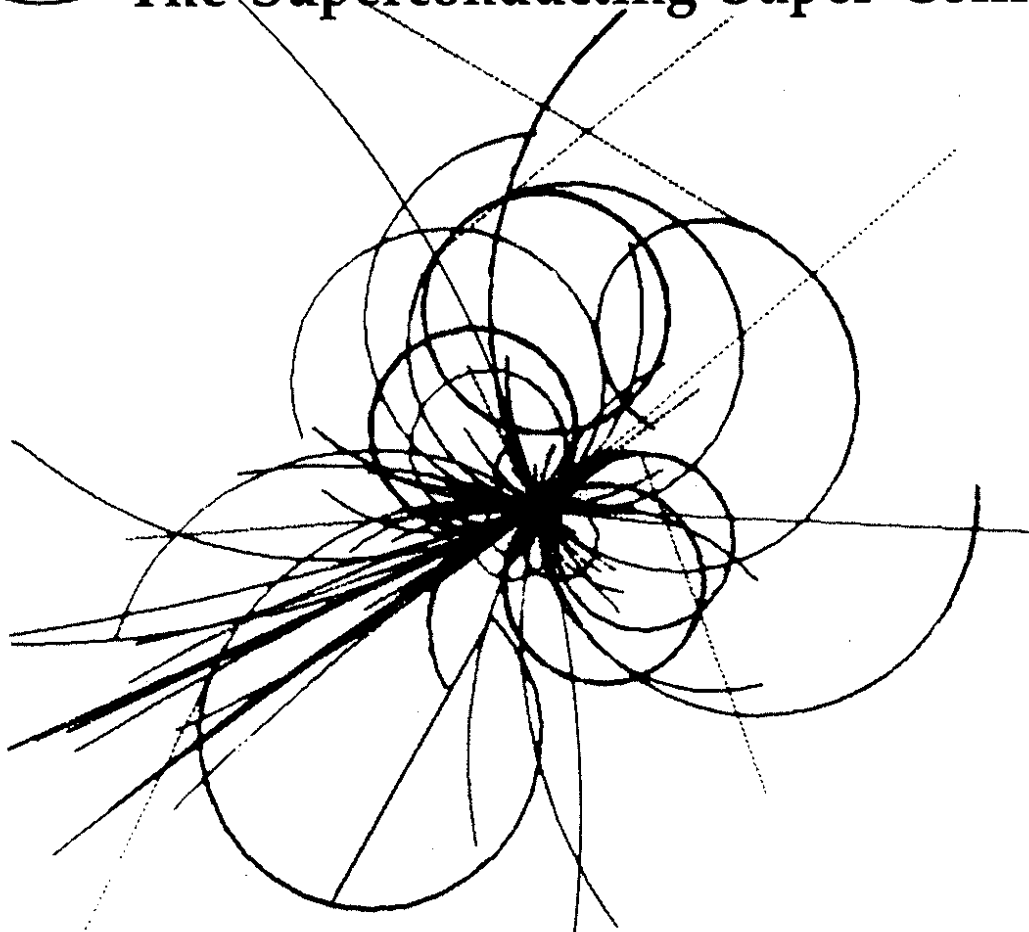




The Superconducting Super Collider



Empirical Hamiltonians

S. Peggs and R. Talman
SSC Central Design Group

August 1986

EMPIRICAL HAMILTONIANS*

S. Peggs and R. Talman
SSC Central Design Group[†]
c/o Lawrence Berkeley Laboratory
Berkeley, California 94720

August 1986

*Submitted to the 13th International Conference on High Energy Accelerators,
Novosibirsk, USSR, 7-11 August 1986

[†]Operated by Universities Research Association, Inc. for the U. S. Department
of Energy

EMPIRICAL HAMILTONIANS

S. Peggs and R. Talman *
SSC Central Design Group *
LBL, 1 Cyclotron Road
Berkeley California 94720, USA

Introduction

As proton accelerators get larger, and include more magnets, the conventional tracking programs which simulate them run slower. At the same time, in order to more carefully optimise the higher cost of the accelerators, they must return more accurate results, even in the presence of a longer list of realistic effects, such as magnet errors and misalignments. For these reasons conventional tracking programs continue to be computationally bound, despite the continually increasing computing power available. This limitation is especially severe for a class of problems in which some lattice parameter is slowly varying, when a faithful description is only obtained by tracking for an exceedingly large number of turns. Examples are synchrotron oscillations in which the energy varies slowly with a period of, say, hundreds of turns, or magnet ripple or noise on a comparably slow time scale. In these cases one may wish to track for hundreds of periods of the slowly varying parameter.

The purpose of this paper is to describe a method, still under development, in which element-by-element tracking around one turn is replaced by a single map, which can be processed far faster. Similar programs have already been written in which successive elements are "concatenated" with truncation to linear, sextupole, or octupole order, et cetera, using Lie algebraic techniques to preserve symplecticity[1,2]. The method described here is rather more empirical than this but, in principle, contains information to all orders and is able to handle resonances in a more straightforward fashion.

It is assumed for this method that a conventional program exists which can perform faithful tracking in the lattice under study for some hundreds of turns, with all lattice parameters held constant. An empirical map is then generated by comparison with the tracking program. There is no pretense at rigor - the empirical map is only judged to give a sufficiently accurate representation of the supposedly exact tracking data. Having replaced the true motion by an empirical map with very similar features (that is, containing the "physics") we again have a well posed mathematical problem of the influence of modulating the parameters of the map. The way this modulation is performed is described below.

Certain features, such as chaos on a microscopic scale, will not be faithfully represented, but an example will be given showing that this can be unimportant, and that the physically interesting behavior only emerges after parametric modulation is introduced. The empirical Hamiltonian approach is applied to the example, giving an excellent representation of the true motion, which is dramatically affected by the modulation. At present, and as described here, the software tools to carry out the derivation of the map, and to track using it, only work in one transverse dimension. It is hoped that they can be extended to two transverse dimensions in the near future.

Resonant Invariants and Empirical Hamiltonians

Suppose that the conventional tracking program is used to determine the horizontal physical coordinates, x_n and x'_n , of a fixed energy test particle on turn number n , for many successive turns. While these programs naturally use Cartesian coordinates, it is convenient to present the data graphically in polar coordinates of amplitude and phase, a_n and ψ_n , where

$$x_n = a_n \sin(\psi_n), \quad x'_n = a_n [\cos(\psi_n) - \alpha \sin(\psi_n)] / \beta \quad (1)$$

and α and β are Twiss parameters at the reference point. If no nonlinearities are present in a (a_n, ψ_n) phase space scatter plot, all the points will lie on a straight line of constant amplitude a_n , but successive points will be spaced in ψ by $2\pi Q$, where Q is the tune. For sufficiently small amplitudes and neglecting small chaotic regions, the points in a scatter plot still lie on a definite "invariant" line when nonlinearities are introduced. The line is in general curved, and may even close on itself in a discrete set of "islands".

*Operated by the Universities Research Association for the U.S. Department of Energy.

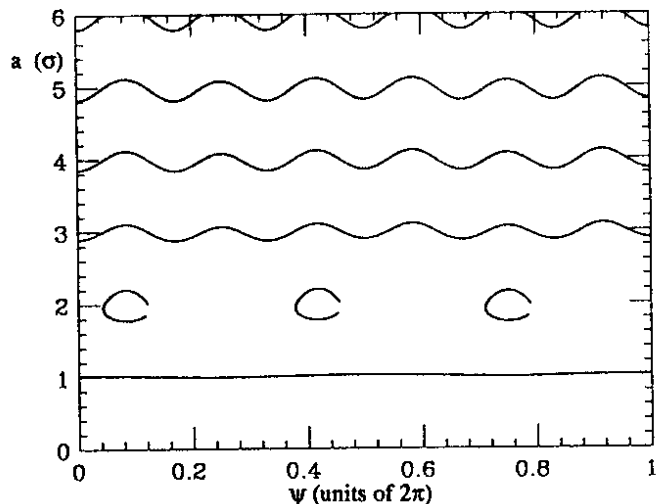


Figure 1 The phase space trajectories of six particles, perturbed by a single round beam-beam collision per turn of strength $\xi=0.0042$, followed for 970 turns with a conventional tracking program around a machine with an unperturbed tune of $Q_0=0.331$.

Figure 1 shows the phase space motion of six trajectories followed for 970 turns, with a single beam-beam interaction of tune shift parameter $\xi = 0.0042$ encountered once per turn. It is natural to plot the measured amplitude a in units of σ , the gaussian size of the round opposing beam. The tune approaches its unshifted value of $Q_0 = 0.331$ at large amplitudes, and at small amplitudes approaches $Q_0 + \xi = 0.3352$, so that the tune distribution is spread across the sixth order, $Q = 2/6$, resonance. (The symmetry of the idealised beam-beam kick disallows the $Q = 1/3$ and all other odd order resonances.) Abstract general comments will be illustrated at several points below by continued references to this particular example.

The trajectory in figure 1 with an amplitude $a \approx 2\sigma$ exhibits resonance lock on. This particle jumps from one island to the next but one on every turn, to visit only three of the six equivalent islands. No particle was launched on the other three islands, and so they do not appear. If the trajectory is plotted every three turns, the successive points appear to march slowly around a single island, with a period somewhat larger than 970 turns. These points are so close together that, to the resolution of the figure, they form a continuous invariant curve. Similarly, if only every third point of a nonresonant trajectory is plotted, the progress across the figure is also slow, with an average phase advance per three turns of

$$\langle \Delta_3 \psi \rangle = 3 \cdot 2\pi \cdot (Q(a) - 1/3) \quad (2)$$

which is proportional to the average tune separation from the resonance.

Although all of the trajectories shown in the figure are "regular", some initial conditions lead to "chaotic" behavior, in which successive points appear to wander randomly over a bounded region of phase space, instead of lying on smooth invariant curves. This kind of behavior will be neglected for now and discussed further below. The curves followed by regular trajectories (for example those in figure 1) can be described as contours of an "invariant function", H_I , which can in general be decomposed into Fourier harmonics as

$$H_I(J, \phi) = U(J) + \sum_{m=1}^{\infty} V_m(J) \cdot \cos[m(\psi - \phi_m(J))] \quad (3)$$

where the functions $U(J)$, $V_m(J)$ and $\phi_m(J)$ are independent of time. Here the $m=0$ term, $U(J)$, has been defined separately for later convenience, and the action coordinate J has been introduced;

its value on the n'th turn is

$$J_n = 1/2 a_n^2 \quad (4)$$

The function H_I is not unique; if the right hand side of (3) is multiplied by a constant the contours of the new function are unchanged. This ambiguity will now be removed, in the process of treating H_I as a true Hamiltonian.

Though the coordinates x_n, x'_n or equivalently J_n, ψ_n are determined only for integer values of n , we now introduce a continuous time variable t , which increases by one unit for each turn around the accelerator. The action-angle variables $J(t)$ and $\psi(t)$ are assumed to vary with time according to

$$\frac{d\psi}{dt} = \frac{\partial H_k}{\partial J}, \quad \frac{dJ}{dt} = -\frac{\partial H_k}{\partial \psi} \quad (5)$$

where k is an integer such that the tune of all particles is near j/k , with j being another integer. The "empirical Hamiltonian" $H_k(J, \psi)$ is one of the functions H_I , with the previously undefined multiplicative constant chosen to make (5) best agree with (1) after integration over k units of time.

It can be seen that the motion defined in this way is completely artificial for non integer values of t , and even for integer values which do not divide by k . The values taken on by $J(t)$ and $\psi(t)$ are unrelated to the values of J and ψ actually taken on by a particle as it proceeds around the accelerator. Rather they are smooth interpolations between the discrete values taken on every k 'th turn. One can simply imagine the phase point slowly moving along the invariant curves, such as those of figure 1. (Recall that $j=1, k=3$ for this standard example.)

In the particular case that only the Fourier term $m=k$ is present in (3), this procedure is equivalent to changing to a comoving frame, where the phase $\psi - (j/k) 2\pi n$ advances only slowly with turn number. However, in practical situations, and even in the simple example being demonstrated here, it is necessary to include more than one Fourier term in order to closely match the data found by tracking.

Numerical Determination of Empirical Hamiltonians

The functions $U(J)$, $V_m(J)$, and $\phi_m(J)$ are "guessed" as simple analytic functions having free parameters, which are determined by matching the empirical motion to the motion given by the tracking program. To do this the vector empirically describing motion in phase space over k turns, $(\Delta_k J, \Delta_k \psi)$, is first approximated by combining (3) and (5) to give

$$\Delta_k \psi / k \approx \partial H_k / \partial J \approx U'(\langle J \rangle) + 1/2 U''(\langle J \rangle) \cdot (J - \langle J \rangle) + \sum_m V'_m(\langle J \rangle) \cos[m(\psi - \phi_m(\langle J \rangle))] \quad (6)$$

and

$$\Delta_k J / k \approx -\partial H_k / \partial \psi \approx \sum_m m V_m(\langle J \rangle) \sin[m(\psi - \phi_m(\langle J \rangle))] \quad (7)$$

in a Taylor expansion about $\langle J \rangle$, the mean action. A prime signifies differentiation by J . A presumably negligible term in $\phi'_m(\langle J \rangle)$ has been dropped in (6), while the term in $U''(\langle J \rangle)$ has been added to allow for the possibility that motion is resonant, in which case H_k has a local minimum or maximum.

The quantities $U'(\langle J \rangle)$, $V'_m(\langle J \rangle)$ and $\phi'_m(\langle J \rangle)$ in (6) and (7) are treated as parameters which are varied to best fit the observed data for a single trajectory, for example by minimising the sum

$$S = \sum (\Delta_k J_{\text{fit}} - \Delta_k J_{\text{data}})^2 + (\Delta_k \psi_{\text{fit}} - \Delta_k \psi_{\text{data}})^2 \quad (8)$$

If the data come from tracking for N turns, there are $N-k$ values in the sum. This works for both resonant and nonresonant trajectories, but assumes that a small number of important Fourier harmonics have been identified ahead of time. The parameters of the analytic guesses for $U(J)$, $V_m(J)$, and $\phi_m(J)$ are then adjusted to best fit the set of values for $U'(\langle J \rangle)$, $V'_m(\langle J \rangle)$ and $\phi'_m(\langle J \rangle)$ which have been determined for each value of $\langle J \rangle$, that is, for each trajectory.

The process of empirical Hamiltonian determination is now demonstrated by pursuing the standard beam-beam example further. Figure 2 plots the $a=3\sigma$ trajectory already drawn in figure 1, but on an expanded scale, showing that the $m=2$ and $m=6$ terms are dominant in the Fourier series. Only these two harmonics will be retained.

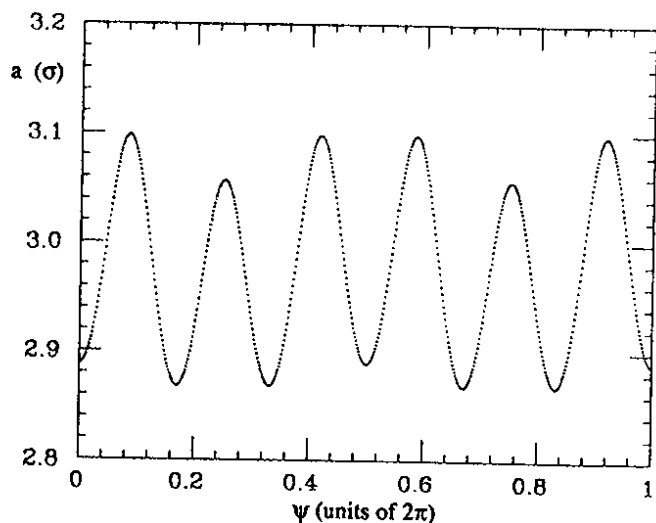


Figure 2 The trajectory $a=3\sigma$ of figure 1, plotted on an expanded scale, showing the dominance of $m=2$ and 6 harmonics.

Figure 3 shows the six values of U' found by fitting each of the trajectories in figure 1 as crosses, and shows the analytic approximation to U' , a Pade approximation, as a solid curve. The dashed line shows the behavior of U' expected on purely theoretical grounds[3,4] in a comoving frame analysis. Similarly, figure 4a shows the individual fits, the analytic approximation, and the theoretical prediction for V_6 as crosses, a solid line, and a dashed line. Figure 4b shows the results of a straight line fit (in amplitude) of ϕ_6 as a solid line. In theory ϕ_6 is expected to be $-\pi/6$, and constant. Although the agreement does not appear to be very good, it should be noted that the vertical scale is quite expanded. The empirical tracking results shown below are insensitive to this fit, and to the ϕ_2 fit shown below, both of which could easily be improved. Finally, figures 5a and 5b show the individual fits of V_2 and ϕ_2 , and their analytical approximations by straight lines (in amplitude). In the theoretical comoving frame analysis of this simple example all terms other than V_6 are explicitly dropped, a procedure which is justified by comparing figures 4a and 5a, and noting that V_2 is relatively small.

Table 1 summarises the situation, showing the theoretical behavior and the analytic Pade approximations for all of the functions. I_n is a reduced Bessel function of order n .

Function	Theory	Analytic Fit
U'	$\frac{1}{2} [1 - e^{-J/2} I_0(J/2)] + \text{constant}$	$-0.0152 + \frac{0.0280}{1 + 0.463 J}$
V_6	$\int \frac{4}{J} e^{-J/2} I_3(J/2) dJ$	$\frac{4.08 \cdot 10^{-5} J^3 + 4.37 \cdot 10^{-6} J^5}{1 + 4.82 \cdot 10^{-2} J^3 + 2.62 \cdot 10^{-4} J^5}$
ϕ_6	$-\pi/6$	$-0.531 + 4.91 \cdot 10^{-3} J^{1/2}$
V_2	—	$4.14 \cdot 10^{-4} + 3.54 \cdot 10^{-4} J^{1/2}$
ϕ_2	—	$5.47 \cdot 10^{-3} - 1.12 \cdot 10^{-3} J^{1/2}$

Table 1 Theoretical behavior and analytic fits for the functions in the empirical Hamiltonian representing the beam beam example.

Tracking with Empirical Hamiltonians

An empirical Hamiltonian can be found at any fixed value of a parameter, for example the energy offset $\delta = \Delta E/E$, using the procedures described above, provided only that displacements are measured about the true closed orbit. A global empirical Hamiltonian, valid over a range of the parameter, may then be constructed by fitting parametric functions like $U(J, \delta)$ to a small

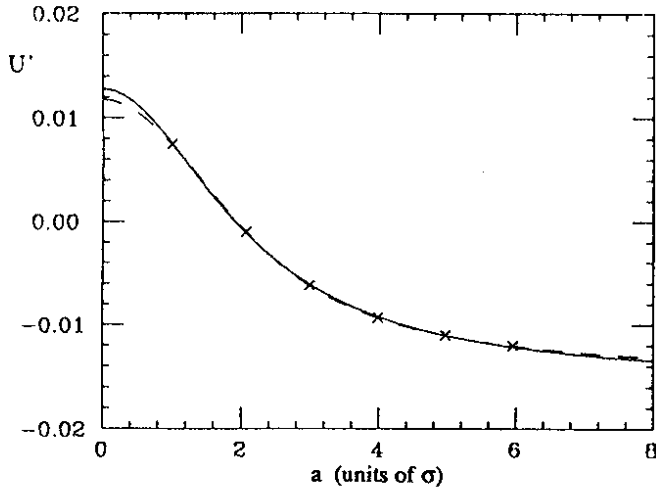


Figure 3 The values of U' found by fitting each of the six trajectories in figure 1 (crosses), as fit by a Pade approximation (solid curve), and according to theory (dashed curve).

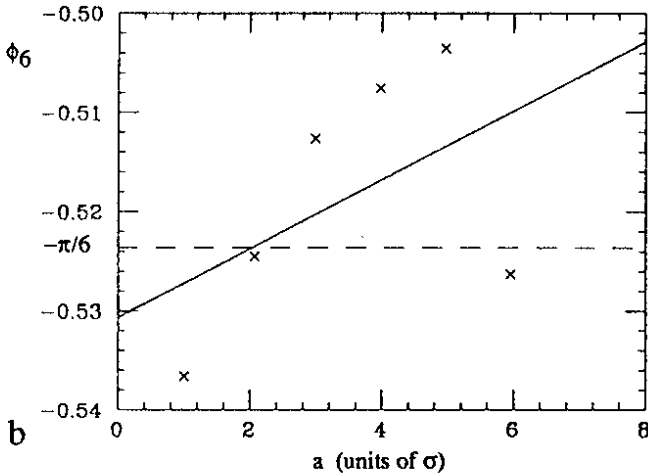
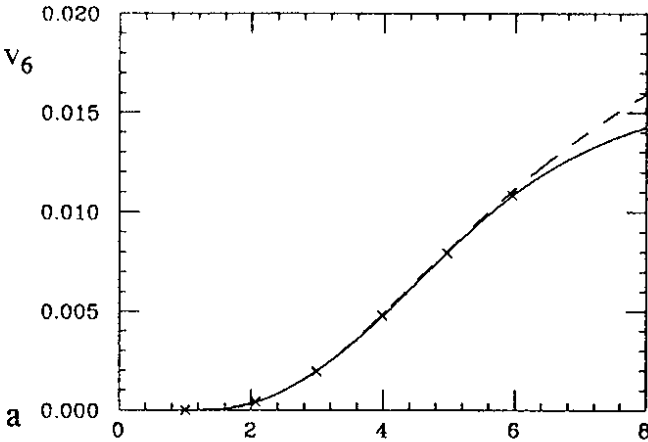


Figure 4 The values of (a) V_6 and (b) ϕ_6 found by fitting each of the six trajectories in figure 1 (crosses), fit by Pade approximations (solid curves), and according to theory (dashed curves).

number of these particular maps. Tracking is performed by keeping the parameter constant for one turn, and using a numerical algorithm representing the integration of (5), referred to the current value of the parameter. The parameter is adjusted after every turn as appropriate - in the case of synchrotron oscillations δ is varied sinusoidally and inexorably, mimicking an idealised thin radio frequency cavity at the reference point.

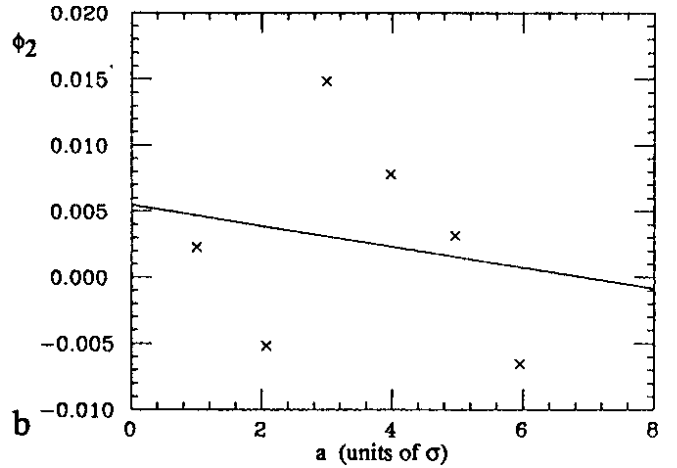
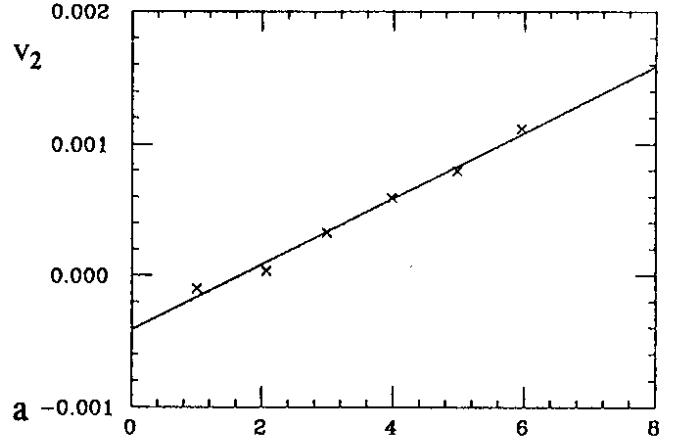


Figure 5 The values of (a) V_2 and (b) ϕ_2 found by fitting individual trajectories in figure 1 (crosses), and as fit globally by linear functions of amplitude.

It is essential that the value of H_k at the new phase space location, after single turn propagation using the numerical algorithm, is exactly the same as at the old, so that

$$H_k(J_{\text{new}}, \Psi_{\text{new}}) = H_k(J_{\text{old}}, \Psi_{\text{old}}) \quad (9)$$

In the results presented below the second condition in the algorithm makes the square of the path length of the propagation line segment $(\Delta J, \Delta \Psi)$ the average of the "old" and "new" Hamiltonian slopes.

$$\Delta J^2 + \Delta \Psi^2 = \frac{1}{2} \left[\left(\frac{\partial H^2}{\partial \Psi_{\text{old}}} + \frac{\partial H^2}{\partial J_{\text{old}}} \right) + \left(\frac{\partial H^2}{\partial \Psi_{\text{new}}} + \frac{\partial H^2}{\partial J_{\text{new}}} \right) \right] \quad (10)$$

Equations (9) and (10) are symmetric with respect to initial and final coordinates, making the motion reversible.

We now use the empirical Hamiltonian method to track particles in the presence of synchrotron oscillations, for comparison with exact tracking results. Figure 6a plots one phase space point at the end of each of 1000 synchrotron oscillations, in the standard beam-beam example with $\xi=0.0042$, for many different initial conditions. The unperturbed tune is modulated at the synchrotron frequency, so that on turn n

$$Q = Q_0 + q \cos(2\pi Q_s n) \quad (11)$$

where the base tune is $Q_0 = 0.331$, the tune modulation amplitude is $q = 0.001$, and the synchrotron tune is $Q_s = 1/194$. A family of synchrotron sidebands of the main resonance appears when tune modulation is included[3,4], corresponding to the shifted tunes

$$Q(a) = 2/6 + p \cdot Q_s / 6 \quad (12)$$

where p is an integer. The $p = 1, 0, -1$, and -2 sidebands are clearly visible. Chaos ensues when these sidebands overlap[5], that is, when the beam-beam tune shift parameter ξ is raised so that the islands are more narrowly spaced in amplitude. The parameters of the example have been carefully chosen to show the onset of chaos, especially between the $p = 0$ and -1 sidebands. If the tune shift parameter is increased to 0.006, the entire region from $a=2\sigma$ to $a=6\sigma$ becomes chaotic[4].

Figure 6b reproduces the results of 6a by tracking with the one turn propagation algorithm described above, based on the empirical Hamiltonian described in figures 3, 4, and 5. Instead of parameterising the Hamiltonian with energy, however, the tune modulation was added as a second mapping, adding a small amount of oscillating phase advance after each single turn propagation. The two figures are not exactly identical in their features, despite using exactly the same initial conditions for each trajectory, but they agree very well in the size of the sidebands, and in the presence of chaotic behavior in some regions.

Conclusions and Potential Applications

A procedure has been outlined for determining an empirical Hamiltonian, which can represent motion through many nonlinear kicks, by taking data from a conventional tracking program. Though derived by an approximate method this Hamiltonian is analytic in form and can be subjected to further analysis of varying degrees of mathematical rigor. Typical fields for study include:

- i) Many potential uses in long term tracking studies. The example of this paper shows that the large scale chaos induced by synchrotron oscillations in the presence of a single beam beam interaction is well accounted for by the empirical Hamiltonian method.
- ii) The importance of microscopic chaos in the original map. Even a modulation free nonlinear map is known to have small chaotic regions which are not included in our empirical map. It may be possible to neglect these regions altogether, for practical purposes, if modulation sources causing much more extreme chaos are present. An example showing such behavior has been given.
- iii) A more detailed application of the Chirikov criterion, or a more rigorous analysis of the time-varying Hamiltonian. The modulation free Hamiltonian H_k can, according to (3) and (5), be written as

$$H_k(J, \phi) = 2\pi Q_0 J + W(J) + \sum_{m=1}^{\infty} V_m(J) \cdot \cos[m(\psi - \phi_m(J))] \quad (13)$$

where all the terms are proportional to the perturbation strength, except for one, $2\pi Q_0 J$, which involves the unperturbed tune. Synchrotron oscillations cause Q_0 to be replaced by the modulated tune Q given by (11), making H_k time dependent. Various authors[3,4,5,6] have described the model of "sideband island chains" caused by this modulation, and the chaos which accompanies their overlap. The chaotic behavior observed in figure 6 is qualitatively well understood in these terms. This model has so far been restricted to describing sidebands close to a single dominant island chain, but the empirical approach should lead to a more globally accurate description, since the functions in (13) have been selected to give a good description for a broad range of amplitudes.

Even though the empirical procedure has only been described here in one transverse dimension, there is good reason to hope that it can be extended to include two transverse dimensions, so that it can become a more practical tool in realistic cases. The numerical codes which at the time of writing only deal with horizontal motion need to be extended to include vertical motion, and to include a more general parametric variation of the one turn map.

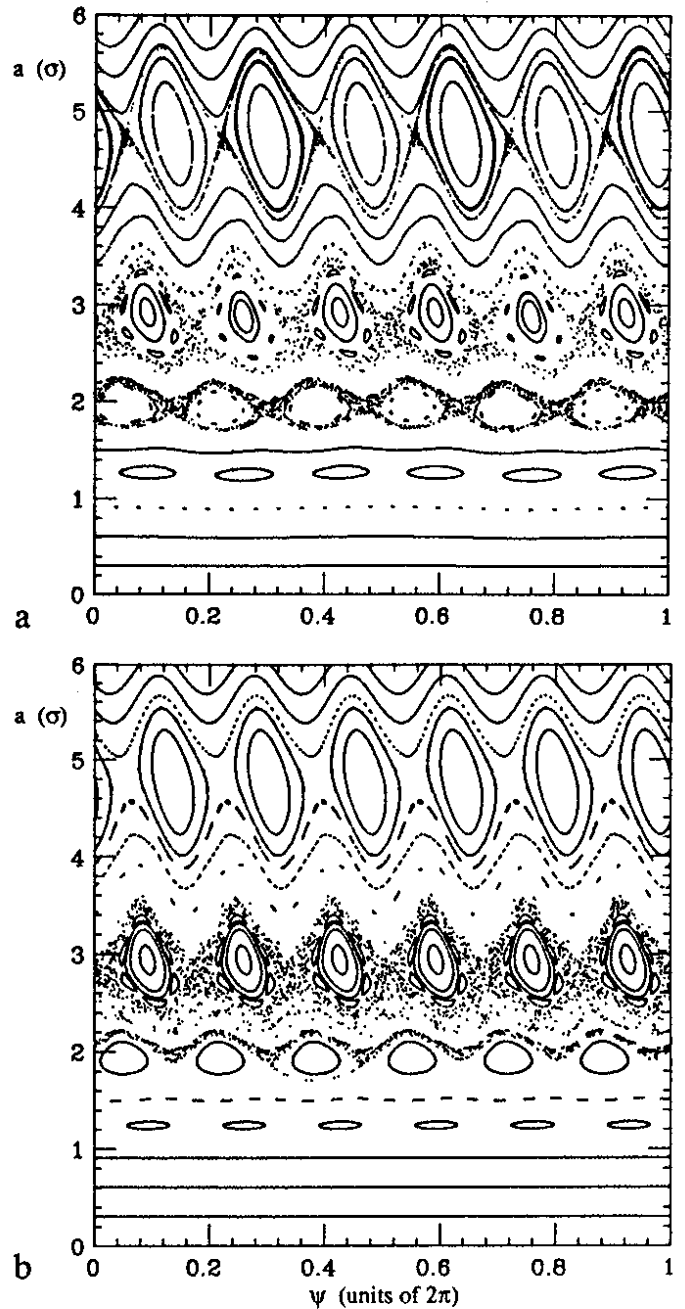


Figure 6 Trajectories followed for 1000 synchrotron periods of 194 turns (a) by conventional tracking, and (b) using the empirical Hamiltonian of Table 1. Apart from the addition of tune modulation with an amplitude $q=0.001$, the model is the same as in figure 1. One point is plotted at the end of every synchrotron period.

References

1. See for example Douglas, D., Dragt, A. 1983. *Proc. 12th Int. Conf. on High Energy Accelerators*, Fermilab, Batavia, Illinois
2. Forest, E. 1986. Unpublished.
3. Evans, L. 1981. *CERN SPS/81-2*, CERN, Geneva
- Evans, L., Gareyte, J. 1982. *IEEE Trans. Nucl. Sci.*, NS-30 : 4
- Evans, L. 1983. *CERN SPS/83-38*, CERN, Geneva
4. Peggs, S., Talman, R. 1986. *SSC-61*, SSC Central Design Group, Berkeley, California
5. Chirikov, B. 1979. *Phys. Reports*, 52 : 265
6. Peggs, S. 1985. *Particle Accelerators*, 17 : pp. 11-50

